Synthesis and Photovoltaic Properties of Novel Ruthenium(II) Sensitizers for Dye-sensitized Solar Cell Applications

Tae In Ryu, Myungkwan Song, Myung Jin Lee, Sung-Ho Jin,[*] Sunwoo Kang,[†] Jin Yong Lee,[†] Jae Wook Lee,[‡,*] Chan Woo Lee,[§] and Yeong-Soon Gal[#]

Department of Chemistry Education, Interdisciplinary Program of Advanced Information and Display Materials, and Center for Plastic Information System, Pusan National University, Busan 609-735, Korea. [*]E-mail: shjin@pusan.ac.kr
[†]Department of Chemistry, Sungkyunkwan University, Suwon 440-746, Korea
[‡]Department of Chemistry, Dong-A University, Busan 604-714, Korea. [*]E-mail: jlee@donga.ac.kr
[§]Department of Chemistry, University of Ulsan, Ulsan 680-749, Korea
[#]Polymer Chemistry Lab, Kyungil University, Hayang 712-701, Korea
Received July 15, 2009, Accepted August 24, 2009

Three heteroleptic ruthenium sensitizers, $Ru(L)(L^1)(NCS)_2$ [L = 4,4'-dicarboxylic acid-2,2'-bipyridine, **Ru-T1**: L^1 = (E)-2-(4'-methyl-2,2'-bipyridin-4-yl)-3-(thiophen-2-yl)acrylonitrile, **Ru-T2**: L^2 = (E)-3-(5'-hexyl-2,2'-bithiophen-5-yl)-2-(4'-methyl-2,2'-bipyridin-4-yl)acrylonitrile, and **Ru-T3**: L^3 = (E)-3-(5"-hexyl-2,2':5',2"-terthiophen-5-yl)-2-(4'-methyl-2,2'-bipyridin-4-yl)acrylonitrile)], were synthesized and used as photosensitizers in nanocrystalline dye-sensitized solar cells (DSSCs). The introduction of the 3-(5-hexyloligothiophen-5-yl)acrylonitrile group increased the conjugation length of the bipyridine donor ligand and thus improved their molar absorption coefficient and light harvesting efficiency. DSSCs with the configuration of SnO_2: F/TiO_2/ruthenium dye/liquid electrolyte/Pt devices were fabricated using these **Ru-T1** ~ **T3** as a photosensitizers. Among the devices, the DSSCs composed of **Ru-T2** exhibited highest power conversion efficiency (PCE) of 2.84% under AM 1.5 G illumination (100 mW/cm^2).

Key Words: Ruthenium sensitizer, Oligothiophene, Dye-sensitized solar cell

Introduction

The effective conversion of solar energy into electricity has become a very important issue in the last few years due to rising energy costs and demand.[1] In recent years, dye-sensitized solar cells (DSSCs) based on nanocrystalline TiO_2 (nc-TiO_2) films have received significant attention because of their high efficiency and low cost compared to those of silicon solar cells.[2-3] In addition to the possibility of low production cost, another important advantage over conventional solar cells is the versatile design possibilities, such as production of flexible DSSCs with variable colors. In DSSCs, the sensitizing dye molecules must be chemically adsorbed on the porous nc-TiO_2 surfaces and be capable of harvesting solar light ranging from the visible to the near-IR regions. Up to now, the efficient sensitizers that have received the most research attention are ruthenium sensitizers[4] which show effective charge separation at the metal to ligand (Ru-bpy) and ligand to metal (SCN-Ru) absorption bands in the visible solar light region. Although a variety of sensitizers, including metal-free organic dyes and non-ruthenium metal dyes, have been used, ruthenium polypyridine sensitizers exhibit the best performance to date.[5-7] With regard to the sensitizers, several ruthenium polypyridine sensitizers, such as cis-dithiocyanato bis(4,4'-dicarboxy-2,2'-bipyridine)ruthenium(II) (N3),[2-3] its bis(tetrabutylammonium) salt (N719),[8-9] and trithiocyanato (4,4',4"-tricarboxy-2,2':6',2"-terpyridine)ruthenium(II) (black dye)[4,10] gave the best power conversion efficiency (PCE) of the examined dyes for DSSCs.

The ruthenium sensitizers underwent molecular engineering to maximize the PCE and thereby increase the molar absorption coefficient and reduce the number of protons on the complexes. 4,4'-Dicarboxylic acid-2,2'-bipyridine (dcbpy) has been considered the best anchoring ligand in Ru sensitizers.[11] Replacement of one of the dcbpy anchoring ligands was reported by Grätzel and coworkers as a molecular engineering approach for increasing the molar absorption coefficient and the photocurrent density of the sensitizers.[12-13] One strategy for increasing the light harvesting efficiency is to increase the conjugation length of the ligand.[14-16] For example, various types of alkyloligothiophene and vinylene units are introduced into the bipyridine (bpy) ligand as a pendant group.

In this paper, we design and synthesize of a new series of heteroleptic ruthenium sensitizers containing (E)-3-(5-hexyloligothiophen-5-yl)-2-(4'-methyl-2,2'-bipyridin-4-yl)acrylonitrile ligands (L^1, L^2, L^3), in place of dcbpy, in a ruthenium sensitizers. The sensitizers exhibit improved molar absorption coefficient while maintaining the required thermal and photostability. The new side chains are introduced on the bipyridine unit, in order to increase the conjugation length and thereby improve the light harvesting efficiency. We describe their thermal, optical, electrochemical properties, and photovoltaic properties.

Experimental Section

Materials. Selenium dioxide (SeO_2), 4,4'-dimethyl-2,2'-bipyridine, sodium borohydride, sodium hydroxide, sodium carbonate, 18-crown-6, potassium cyanide, *N*-bromosuccinimide (NBS), 2-thiophenecarboaldehyde, tetrakis(triphenylphosphine) palladium(0), [Ru(*p*-cymene)Cl_2]$_2$, 4,4'-dicarboxylic acid-2,2'-bipyridine, ammonium thiocyanate were purchased from Aldrich

Chemical Co. and TCI organic chemicals. These were used without further purification unless otherwise noted. Solvents were dried and purified by fractional distillation over sodium/benzophenone and handled in moisture free atmosphere. *N*,*N*-dimethylformamide (DMF) was stirred with anhydrous $MgSO_4$ for overnight and distilled under reduced pressure. Column chromatography was performed using silica gel (Merck, 250 ~ 430 mesh) and using Sephadex LH-20 (GE Healthcare).

Instruments. ^{1}H-NMR spectra were recorded in $CDCl_3$ on a Varian Mercury 300, and chemical shifts were recorded in ppm. The absorption spectra were measured using a Jasco V-570 UV-visible spectrometer. IR spectra were measured using a EQUINOX55 FTIR spectrometer. Thermal analyses were carried out on a Mettler Toledo TGA/SDTA 851e, DSC 822e analyzer under a nitrogen atmosphere at a heating rate of 10 ^{o}C/min. Density functional theory (DFT) calculations employing the Becke's three parameters employing Lee-Yang-Parr exchange functional (B3LYP) with 3-21 G* basis sets using a suite of Gaussian 03 programs.[17] Cyclic voltammetry (CV) was carried out with a Bioanalytical Systems CV-50 W voltametric analyzer at a potential scan rate of 100 mV/s in a 0.1 M solution of tetrabutylammonium perchlorate in anhydrous DMF. Each complexes, **Ru-T1**~**T3** were absorbed on TiO_2 coated FTO glass using electrode (4 cm^2) by dipping the TiO_2 coated FTO glass into complexes solution. A platinum wire was used as the counter electrode and an Ag/$AgNO_3$ electrode was used as the reference electrode. All of the electrochemical experiments were performed in a glove box under an N_2 atmosphere at room temperature.

Synthesis of 4-hydroxymethyl-4'-methyl-2,2'-bipyridine (1): SeO_2 (9.8 g, 88.3 mmol) was added to a stirred suspension of 4,4'-dimethyl-2,2'-bipyridine (10 g, 54.3 mmol) in 1,4-dioxane (500 mL) under an N_2 atmosphere. The reaction mixture was stirred at reflux for 24 hr. After cooling to room temperature, the mixture was filtered and the solvent was removed in vacuum. The resulting solid was redissolved in chloroform and the suspension was filtered to remove selenium byproducts. After three successive dissolution and filtration treatments, crude product (7 g) was obtained. The resulting solid was suspended in methanol (75 mL) and sodium borohydride (1.5 g) in NaOH (0.2 M, 12.5 mL) was added dropwise to the stirred mixture cooled on ice. The mixture was stirred at room temperature for 2 hr and the methanol was removed in vacuum. The remaining aqueous suspension was diluted with saturated Na_2CO_3 solution (30 mL) and extracted with chloroform. The organic phase was dried and the solvent was evaporated. The crude product was purified by column chromatography (eluent: chloroform/methanol = 15:1) to give 4-hydroxymetyl-4'-methyl-2,2'-bipyridine (**1**) (8.3 g, 77%). ^{1}H-NMR ($CDCl_3$, δ ppm) 8.61 (d, J = 5.1 Hz, 1H), 8.51 (d, J = 4.8 Hz, 1H), 8.32 (s, 1H), 8.20 (s, 1H), 7.30 (d, J = 4.5 Hz, 1H), 7.14 (d, J = 4.5 Hz, 1H), 4.79 (s, 2H), 2.44 (s, 3H). ^{13}C-NMR ($CDCl_3$, δ ppm) 155.7, 155.6, 151.8, 148.9, 148.6, 148.4, 124.7, 122.2, 121.0, 118.6, 62.9, 21.1.

Synthesis of 4-bromomethyl-4'-methyl-2,2'-bipyridine (2): 4-Hydroxymethyl-4'-methyl-2,2'-bipyridine (**1**) (4.6 g, 23 mmol) was dissolved in HBr (48%, 230 mL) and H_2SO_4 (9 mL) was added to the solution. The resulting solution was heated at reflux until all the starting materials had been consumed as monitored by TLC (Al_2O_3 : hexane/EtOAc, 10 : 90). After the reaction had gone to completion, the mixture was cooled to room temperature and then water (65 mL) and dichloromethane (65 mL) were added. The aqueous layer was brought to pH 8 by adding with saturated Na_2CO_3 solution and extracted with dichloromethane (50 mL) until the organic layer was colorless. The combined organic layers were dried with anhydrous $MgSO_4$ and the dichloromethane removed in vacuum to yield 4-bromomethyl-4'-methyl-2,2'-bipyridine (**2**) (5.89 g, 97%).^{1}H-NMR ($CDCl_3$, δ ppm) 8.50 (d, J = 4.8 Hz, 1H), 8.40 (d, J = 4.8 Hz, 1H), 8.29 (s, 1H), 8.10 (s, 1H), 7.16 (d, J = 5.1 Hz, 1H), 6.98 (d, J = 5.1 Hz, 1H), 4.32 (s, 2H), 2.26 (s, 3H). ^{13}C-NMR ($CDCl_3$, δ ppm) 156.5, 154.9, 149.24, 148.6, 147.8, 146.7, 124.6, 123.1, 121.6, 120.6, 30.5, 20.8.

Synthesis of 2,2'-bipyridyl-4'-methyl-4-acetonitrile (3): Finely powdered KCN (6.5 g, 0.1 mol) was added to 4-bromomethyl-4'-methyl-2,2'-bipyridine (**2**) (2.5 g, 9.5 mmol) and 18-crown-6 (0.5 g, 0.19 mmol) in acetonitrile (250 mL), the mixture stirred for 4 hr, diluted with water (100 mL) and extracted with dichloromethane (4 × 75 mL). The combined organic layers were washed with water two more times and then dried over anhydrous $MgSO_4$. After removal the solvent, the residue was subjected to purification by column chromatograph on silica gel (eluent : hexanes/EtOAc = 7 : 3) to give 2,2'-bipyridyl-4'-methyl-4-acetonitrile (**3**) (1.83 g, 92%). ^{1}H-NMR ($CDCl_3$, δ ppm) 8.71 (d, J = 4.8 Hz, 1H), 8.55 (d, J = 4.8 Hz, 1H), 8.40 (s, 1H), 8.26 (s, 1H), 7.37 (d, J = 4.8 Hz, 1H), 7.19 (d, J = 4.5 Hz, 1H), 3.87 (s, 2H), 2.47 (s, 3H). ^{13}C-NMR ($CDCl_3$, δ ppm) 156.4, 154.2, 149.9, 149.0, 148.3, 139.9, 125.2, 122.5, 122.1, 120.5, 23.4, 21.1.

Synthesis of 2-bromo-5-formylthiophene (4): In the absence of light, a solution of NBS (4.8 g, 26.75 mmol) in DMF (25 mL) was added dropwies at room temperature to a well stirred solution of 2-thiophene aldehyde (3 g, 26.75 mmol) in DMF (25 mL). After a 40 hr stirring, the solution was poured onto ice water and extracted several times with diethyl ether. The organic phase was combined, washed with water and the dried over anhydrous $MgSO_4$. The crude product was purified by column chromatography (eluent : chloroform/hexane = 1 : 1) to give 2-bromo-5-formylthiophene (**4**) (4.19 g, 82%). ^{1}H-NMR ($CDCl_3$, δ ppm) 9.61 (s, 1H), 7.34 (s, 1H), 7.01 (s, 1H). ^{13}C-NMR ($CDCl_3$, δ ppm) 181.5, 145.6, 136.7, 131.3, 124.7.

Synthesis of 5-formyl-5'-hexyl-2,2'-bithiophene (6): A mixture of 2-(tri-n-butylstannyl)-5-hexylthiophene (**5**) (8.06 g, 17.62 mmol), 2-bromo-5-formylthiophene (**4**) (3.37 g, 17.62 mmol), and tetrakis(triphenylphosphine)palladium(0) (0.2 g) in dry toluene (165 mL) was heated under N_2. The reaction mixture was refluxed for 24 hr until precipitate formed. After cooling, the solid was collected by filtration and washed several times with hexane, methanol and water. The solid was purified by column chromatography (eluent : chloroform/hexane = 2 : 3) to give 5-formyl-5'-hexyl-2,2'-bithiophene (**6**) (2.6 g, 53%). ^{1}H-NMR ($CDCl_3$, δ ppm) 9.81 (s, 1H), 7.62 (d, J = 3.9 Hz, 1H), 7.16 (d, J = 3.3 Hz, 1H), 7.14 (d, J = 3.9 Hz, 1H), 6.72 (d, J = 3.6 Hz, 1H), 2.79 (t, 1H), 1.65 (m, 2H), 1.31 (m, 7H), 0.91 (m, 3H). ^{13}C-NMR ($CDCl_3$, δ ppm) 182.2, 148.5, 147.6, 140.7, 137.4, 133.1, 125.8, 125.3, 123.2, 31.3, 31.6, 30.3, 28.5, 22.4, 13.9.

Synthesis of 5-bromo-5'-formyl-2,2'-bithiophene (7): In the absence of light, a solution of NBS (2.73 g, 15.34 mmol) in DMF

(20 mL) was added dropwise at room temperature to a solution of 5-formyl-2,2'-bithiophene (2.98 g, 15.34 mmol) in DMF (20 mL). After a 40 hr stirring, the solution was poured onto iced water and extracted several times with diethyl ether. The organic phase were combined, washed with water and dried to yield, after evaporation. The crude product was purified by column chromatography (eluent : chloroform/hexane = 1 : 1) to give 5-bromo-5'-formyl-2,2'-bithiophene (**7**) (3.31 g, 79%). ^{1}H-NMR ($CDCl_3$, δ ppm) 9.84 (s, 1H), 7.65 (d, *J* = 3.9 Hz, 1H), 7.17 (d, *J* = 3.9 Hz, 1H), 7.09 (d, *J* = 3.9 Hz, 1H) 7.02 (d, *J* = 3.9 Hz, 1H).

Synthesis of 5-formyl-5''-hexyl-2,2':5',2''-terthiophene (8): A mixture of 2-(tri-n-butylstannyl)-5-hexylthiophene (**5**) (5.66 g, 12.4 mmol), 5-bromo-5'-formyl-2,2'-bithiophene (**7**) (3.38 g, 12.4 mmol), and tetrakis(triphenylphosphine)palladium(0) (0.2 g) in dry toluene (20 mL) was heated under N_2. The reaction mixture was refluxed for 24 hr until precipitate formed. After cooling, the solid was collected by filtration and washed several times with hexane, methanol and water. The solid was purified by column chromatography (eluent : chloroform/hexane = 1 : 2) to give 5-formyl-5''-hexyl-2,2':5',2''-terthiophene (**8**) (2.5 g, 56%). ^{1}H-NMR ($CDCl_3$, δ ppm) 9.84 (s, 1H), 7.64 (d, *J* = 4.2 Hz, 1H), 7.23 (d, *J* = 3.9 Hz, 1H), 7.19 (d, *J* = 3.9 Hz, 1H), 7.02 (d, *J* = 3.9 Hz, 2H), 6.70 (d, *J* = 3.6 Hz, 1H), 2.79 (t, 1H), 1.68 (m, 2H), 1.33 (m, 7H), 0.89 (m, 3H). ^{13}C-NMR ($CDCl_3$, δ ppm) 182.3, 147.04, 146.71, 141.38, 139.86, 137.29, 133.75, 126.86, 125.03, 124.24, 123.82, 123.79, 31.53, 30.20, 29.22, 28.73, 22.54, 14.04.

Synthesis of (E)-2-(4'-methyl-2,2'-bipyridin-4-yl)-3-(thiophen-2-yl)acrylonitrile (L^1): A mixture of 2,2'-bipyridyl-4'-methyl-4-acetonitrile (**3**) (1 g, 4.78 mmol), 2-thiophene carboaldehyde (0.54 mL, 5.73 mmol), piperidine (10 drops) and freshly distilled toluene (20 mL) were refluxed under N_2 for 24 hr. After cooling, the solution was poured onto water and extracted several times with chloroform. The organic phase was dried with anhydrous $MgSO_4$ and the solvent was evaporated. The crude product was purified by column chromatography (eluent : chloroform/hexane = 1 : 3) to give (E)-2-(4'-methyl-2,2'-bipyridin-4-yl)-3-(thiophen-2-yl)acrylonitrile ($\mathbf{L^1}$) (0.95 g, 66%). ^{1}H-NMR ($CDCl_3$, δ ppm) 8.75 (d, *J* = 5.4 Hz, 1H), 8.67 (d, *J* = 1.5 Hz, 1H), 8.59 (d, *J* = 5.1 Hz, 1H), 8.30 (s, 1H), 8.09 (s, 1H), 7.78 (d, *J* = 3.6 Hz, 1H), 7.68 (d, *J* = 5.7 Hz, 1H), 7.58 (dd, *J* = 2.1 Hz, *J* = 5.25 Hz, 1H), 7.21 (m, 2H), 2.48 (s, 3H). ^{13}C-NMR ($CDCl_3$, δ ppm) 156.7, 154.8, 149.8, 148.7, 148.1, 142.0, 137.1, 136.9, 134.2, 131.8, 128.0, 125.0, 122.0, 120.0, 117.0, 115.9, 105.4, 21.0.

(E)-3-(5'-hexyl-2,2'-bithiophen-5-yl)-2-(4'-methyl-2,2'-bipyridin-4-yl)acrylonitrile ($\mathbf{L^2}$) and 3-(5''-hexyl-2,2':5',2''-terthiophe-5-yl)-2-(4'-methyl-2,2'-bipyridin-4-yl)acrylonitrile ($\mathbf{L^3}$) were synthesized with 2,2'-bipyridyl-4'-methyl-4-acetonitrile (**3**) and various structures of hexyloligothiophene aldehyde using a method similar to that of (E)-2-(4'-methyl-2,2'-bipyridin- 4-yl)-3-(thiophen-2-yl)acrylonitrile ($\mathbf{L^1}$).

(E)-3-(5'-Hexyl-2,2'-bithiophen-5-yl)-2-(4'-methyl-2,2'-bipyridin-4-yl)acrylonitrile (L^2): (0.6 g, 54%). ^{1}H-NMR (300 MHz, $CDCl_3$, δ ppm) 8.73 (d, *J* = 5.1 Hz, 1H), 8.65 (d, *J* = 0.9 Hz, 1H), 8.59 (d, *J* = 5.1 Hz, 1H), 8.29 (d, *J* = 0.6 Hz, 1H), 8.01 (s, 1H), 7.60 (d, *J* = 4.2 Hz, 1H), 7.55 (dd, *J* = 2.1 Hz, *J* = 5.25 Hz, 1H), 7.16 (m, 2H), 6.76 (d, *J* = 3.6 Hz, 1H), 2.83 (t, 2H), 2.48 (s, 3H), 1.71 (m, 2H), 1.35 (m, 6H), 0.91 (m, 3H). ^{13}C-NMR ($CDCl_3$, δ ppm) 156.4, 154.9, 150.0, 148.6, 148.2, 145.0, 142.7, 137.1, 136.3, 135.1, 133.5, 125.6, 125.4, 125.2, 123.3, 122.3, 120.2, 117.4, 116.0, 103.8, 31.5, 31.4, 30.2, 28.7, 23.9, 22.5, 21.2, 13.9.

(E)-3-(5''-Hexyl-2,2':5',2''-terthiophen-5-yl)-2-(4'-methyl-2,2'-bipyridin-4-yl)acrylonitrile (L^3): (0.6 g, 50%). ^{1}H-NMR (300 MHz, $CDCl_3$, δ ppm) 8.82 (s, 1H), 8.70 (d, *J* = 5.1 Hz, 1H), 8.59 (d, *J* = 5.1 Hz, 1H), 8.35 (s, 1H), 8.21 (s, 1H), 7.63 (d, *J* = 3.6 Hz, 1H), 7.55 (d, *J* = 5.1 Hz, 1H), 7.26 (d, *J* = 6 Hz, 1H), 7.22 (d, *J* = 3 Hz, 1H), 7.16 (d, *J* = 3.3 Hz, 1H), 7.00 (d, *J* = 3.9 Hz, 2H), 6.68 (d, *J* = 3.6 Hz, 1H), 2.78 (t, 2H), 2.50 (s, 3H), 1.67 (m, 2H), 1.32 (m, 6H), 0.89 (m, 3H). ^{13}C-NMR ($CDCl_3$, δ ppm) 161.7, 154.7, 150.2, 147.2, 146.5, 144.4, 142.9, 139.4, 137.7, 137.0, 135.6, 133.9, 127.3, 126.5, 125.4, 125.0, 124.1, 123.8, 123.7, 122.9, 120.7, 117.4, 116.4, 103.5, 31.5, 30.2, 28.7, 22.6, 22.5, 21.5, 14.1, 14.0.

Synthesis of Ru(L)(L^1)$(NCS)_2$ (Ru-T1) (where L = 4,4'-dicarboxylic acid-2,2'-bipyridine and L^1 = (E)-2-(4'-methyl-2,2'-bipyridin-4-yl)-3-(thiophen-2-yl)acrylonitrile: [Ru(*p*-cymene)$Cl_2]_2$ (51 mg, 0.17 mmol) and $\mathbf{L^1}$ (51 mg, 0.08 mmol) were dissolved in dry DMF (50 mL). The solution was heated at 80 °C under N_2 for 4 hr in the dark. And then 4,4'-dicarboxylic acid-2,2'-bipyridine (14 mg, 0.06 mmol) was added. The reaction mixture was refluxed at 160 °C for 4 hr. To the resulting solution, ammonium thiocyanate (76 mg, 1 mmol) was added and the reaction mixture was further heated at 130 °C for 4 hr. DMF was removed on a rotary evaporator under vacuum and water (200 mL) was added to induce the precipitate. The resulting solid was filtered off, washed with water and diethyl ether and dried under vacuum. The crude product was dissolved in basic methanol (with TBAOH) and further purified on the Sephadex LH-20 with methanol as an eluent. The main band was collected, concentrated, and precipitated with acidic methanol (HNO_3) to obtain Ru(L)(L^1)$(NCS)_2$ (**Ru-T1**) (22 mg, 49%). Anal. Calcd for $C_{32}H_{21}N_7O_4S_3$: C, 50.25%; H, 2.77%; N, 12.82%; S, 12.58%, Found: C, 52.5%; H, 4.7%; N, 9.5%; S, 6.5%. Ru(L)(L^2)$(NCS)_2$ (**Ru-T2**) (where L = 4,4'-dicarboxylic acid-2,2'-bipyridine and L^2 = (E)-3-(5'-hexyl-2,2'-bithiophen-5-yl)-2-(4'-methyl-2,2'- bipyridin-4-yl)acrylonitrile and Ru(L)(L^3)$(NCS)_2$ (**Ru-T3**) (where L = 4,4'-dicarboxylic acid-2,2'-bipyridine and L^3 = (E)-3-(5''-hexyl-2,2':5',2''-terthiophe-5-yl)-2-(4'-methyl-2,2'-bipyridin-4-yl)acrylonitrile) were synthesized and purified by a method similar to that used for Ru(L)(L^1)$(NCS)_2$ (**Ru-T1**). Ru(L)(L^2)$(NCS)_2$ (**Ru-T2**) (33 mg, 31%). Anal. Calcd for $C_{42}H_{35}N_7O_4S_4$: C, 54.18%; H, 3.79%; N, 10.53%; S, 13.78%, Found: C, 50.3%; H, 3.9%; N, 11.1%; S, 8.3%. Ru(L)(L^3)$(NCS)_2$ (**Ru-T3**) (0.1 g, 53%). Anal. Calcd for $C_{46}H_{37}N_7O_4S_5$: C, 54.53%; H, 3.68%; N, 9.68%; S, 15.82%, Found : C, 51.7%; H, 4.2%; N, 9.6%; S, 9.7%.

DSSC fabrication. DSSC was fabricated using TiO_2 films made from Dyesol titania paste (Dyesol Ltd., Australia). In each case the Dyesol paste was coated on the titanium(IV) isopropoxide pretreated FTO glass using a doctor blade technique. The paste on the FTO was then annealed at 450 °C for 30 min to produce a 13 μm thick nanocrystalline TiO_2 film, unless otherwise specified. The annealed film was impregnated with **Ru-T1** ~ **T3** (0.5 mM) in DMF for 24 hr at room temperature. Each dye-coated film was soaked in DMF for 3 hr to remove unatta-

ched dye molecules and then in absolute ethanol for 2 hr to remove DMF. The resulting ruthenium sensitizer-coated TiO_2 film was washed with ethanol and then used to fabricate the DSSC according to the procedure reported elsewhere.[18] The redox electrolyte solution for a DSSC consisted of 0.05 M I_2, 0.1 M LiI, 0.6 M 1,2-dimethyl-3-hexylimidazolium iodide, and 0.5 M 4-*tert*-butylpyridine in 3-methoxypropionitrile. The active areas of dye-coated TiO_2 films were measured by an image analysis program equipped with a digital microscope camera (Moticam 1000). The performance of DSSCs were measured using a calibrated AM 1.5 G solar simulator (Orel 300 W simulator, models 81150) with a light intensity of 100 mW/cm^2 adjusted using a standard PV reference cell (2 cm × 2 cm monocrystalline silicon solar cell, calibrated at NREL, Colorado, USA) and a computer-controlled Keithley 236 source measure unit.

The PCE (η) of a solar cell given by

$\eta = P_{out}/P_{in} = (J_{sc} \times V_{oc}) \times FF/P_{in}$

with $FF = P_{max}/(J_{sc} \times V_{oc}) = (J_{max} \times V_{max})/(J_{sc} \times V_{oc})$, where P_{out} is the output electrical power of the device under illumination, and P_{in} is the intensity of incident light (e.g., in W/m^2 or mW/cm^2). V_{oc} is the open-circuit voltage, J_{sc} is the short-circuit current density, and fill factor (FF) is calculated from the values of V_{oc}, J_{sc}, and the maximum power point, P_{max}. All fabrication steps and characterization measurements were carried out in an ambient environment without a protective atmosphere. While measuring the current density-voltage (J - V) curves for DSSCs, a black mask was used and only the effective area of the cell was exposed to light irradiation. The data reported in this paper was confirmed by making each device more than 5 times.

Results and Discussion

The electronic and optical properties of ruthenium sensitizers can be controlled by modifying the main ligand's chemical structure. To adjust the highest occupied molecular orbital (HOMO) and lowest unoccupied molecular orbital (LUMO) energy levels and control the formation of amorphous morphology of the ruthenium sensitizers with the aim of improving the photovoltaic performance, we first synthesized heteroleptic ruthenium sensitizers introducing the 3-(5-hexyloligothiophen-5-yl)acrylonitrile into the bipyridine backbone. The synthetic routes for the 2,2'-bipyridyl-4'-methyl-4-acetonitrile (**3**), 5-formyl-5'-hexyl-2,2'-bithiophene (**6**), 5-formyl-5''-hexyl-2,2':5',2''-terthiophene (**8**), and three bipyridyl-based ligands ($\mathbf{L^1}$, $\mathbf{L^2}$, $\mathbf{L^3}$) are described in Scheme 1. The addition of the single 3-(5- hexyloligothiophen-5-yl)acrylonitrile group into the bipyridine chain was expected to tune the HOMO and LUMO energy levels of the

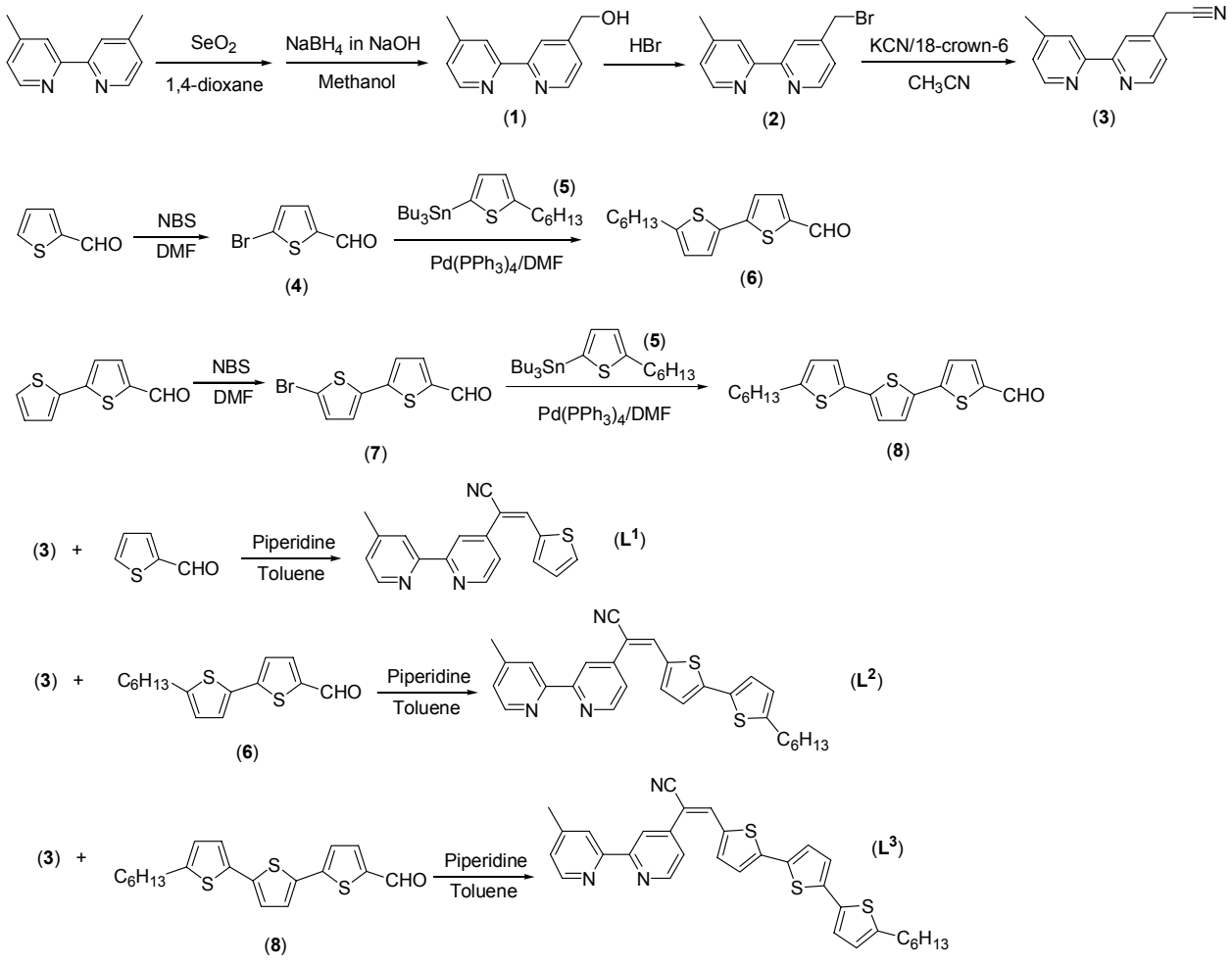

Scheme 1. Synthetic Routes for Ligands.

ruthenium sensitizers as well as amorphous nature due to heteroleptic molecular structures. 4-Hydroxymethyl-4'-methyl-2,2'-bipyridine (**1**) was synthesized by oxidation reaction of 4,4'-dimethyl-2,2'-bipyridine. The bromomethyl compound (**2**) was synthesized by the bromination in acidic solvent. 2,2'-Bipyridyl-4-methyl-4-acetonitrile (**3**) was synthesized by the S_N2 reaction of potassium cyanide in acetonitrile and catalyzed with 18-crown-6. 2-Bromo-5-formylthiophene (**4**) and 2-(tri-n-butylstannyl)-5-hexylthiophene (**5**) were synthesized according to literature procedures.[19] 2-Bromo-5-formylthiophene (**4**) and 5-bromo-5'-formyl-2,2'-bithiophene (**7**) were synthesized by the bromination reaction of 2-thiophenealdehyde and 5-formyl-2,2'-bithiophene with NBS in DMF. 5-Formyl-5'-hexyl-2,2'- bithiophene (**6**) and 5-formyl-5"-hexyl-2,2':5',2"-terthiophene (**8**) were synthesized by the Stille cross-coupling reaction of stannylthiophene (**5**) with compounds (**4**) and (**7**). The newly designed, heteroleptic ligands, $\mathbf{L^1}$, $\mathbf{L^2}$, and $\mathbf{L^3}$, were synthesized by the Knoevenagel reaction with single condensation of hexyloligothiophene aldehydes and 2,2'-bipyridyl-4'-methyl-4-acetonitrile (**3**).

Scheme 2 shows the details of the synthetic methods for the preparation of heteroleptic sensitizers of the type $[Ru(L)(L^x)(NCS)_2]$, where L = 4,4'-bis(carboxylic acid)-2,2'-bipyridine and $L^x = L^1$, L^2, and L^3. Reaction of dichloro(*p*-cymene)ruthenium(II) dimer in DMF at 80 °C with L^x gave a mononuclear complexes. In this step, the substituted bipyridine ligands were coordinated to the ruthenium center with cleavage of the double chloride-bridged structure of the dimeric complex.[20] The heteroleptic dichloro complexes were prepared by reacting the mononuclear $[Ru(L^x)Cl(cymene)]Cl$ complex with L^x under reduced light at 160 °C. The $[Ru(L)(L^x)(Cl)_2]$ complex was reacted with a 20-fold excess of ammonium thiocyanate ligand to obtain the $[Ru(L)(L^x)(NCS)_2]$ sensitizers, **Ru-T1** ~ **T3**.

Ru-T1 ~ **T3** are very weakly soluble in common organic solvents such as acetonitrile, ethanol, methanol, and dichloromethane. However, **Ru-T1** ~ **T3** were sufficiently soluble in DMF and DMSO for their NMR, cyclic voltammetry, and electro-optical properties to be measured. Among **Ru-T1** ~ **T3**, the solubility of **Ru-T2** was higher than that of **Ru-T1** and **Ru-T3**. The structures of the intermediates, ligands, and **Ru-T1** ~ **T3** were confirmed by ^{1}H-, ^{13}C-NMR spectroscopy and elemental analysis.

In general, the ^{1}H-NMR spectra of the ligands show sharp signals in the aromatic region, whereas their corresponding **Ru-T1** ~ **T3** exhibit slightly broader signals. The complicated multiple peaks in the ^{1}H NMR spectrum of **Ru-T1** ~ **T3** indicated that the bipyridine and 3-(5-hexyloligothiophen-5-yl) acrylonitrile moieties were magnetically nonequivalent. The small peak at 9.89 ppm belongs to a portion of carboxylic acid protons, suggesting that the bipyridine ligand contains carboxy-

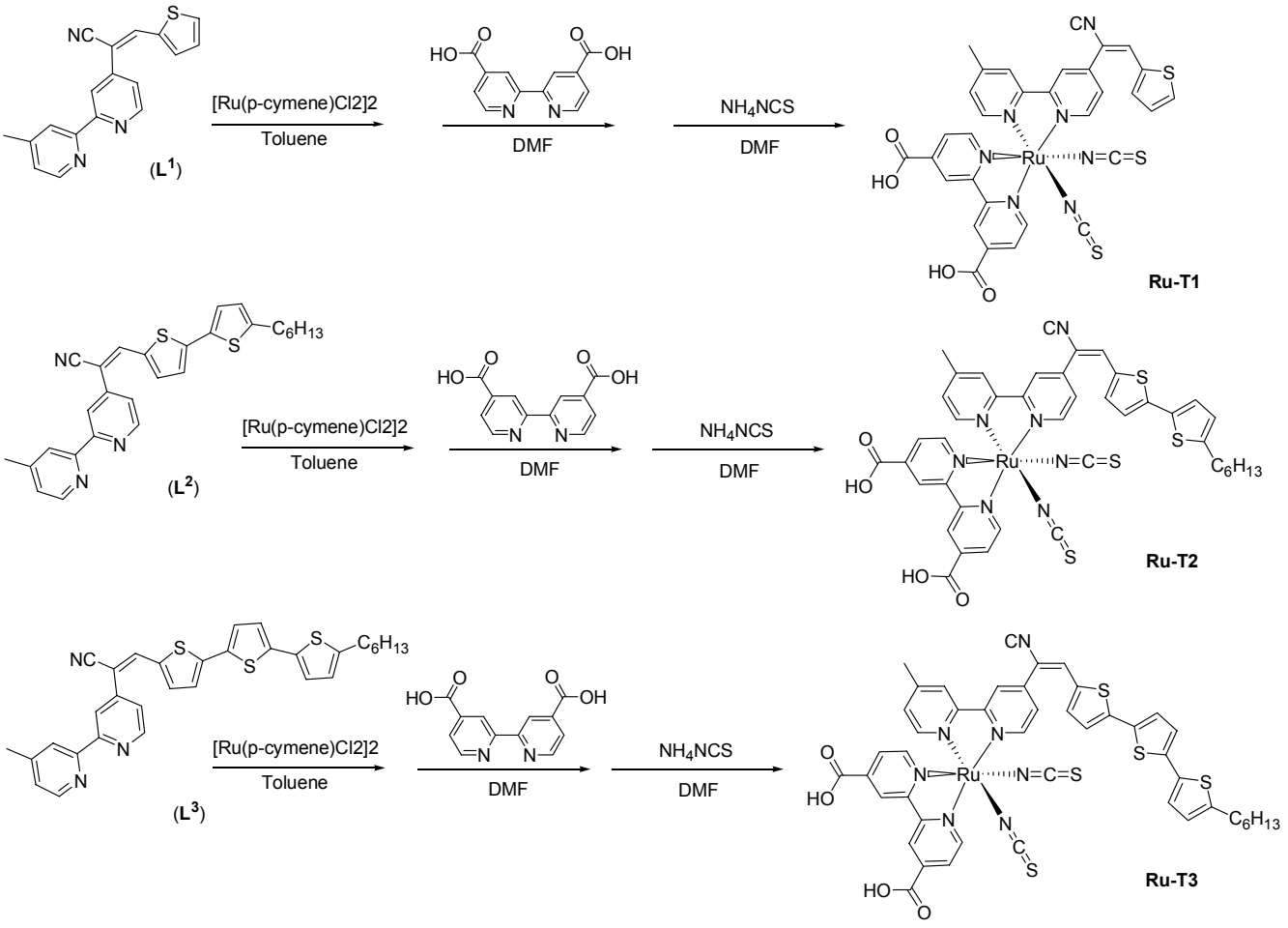

Scheme 2. Synthetic Routes for Ru Sensitizers.

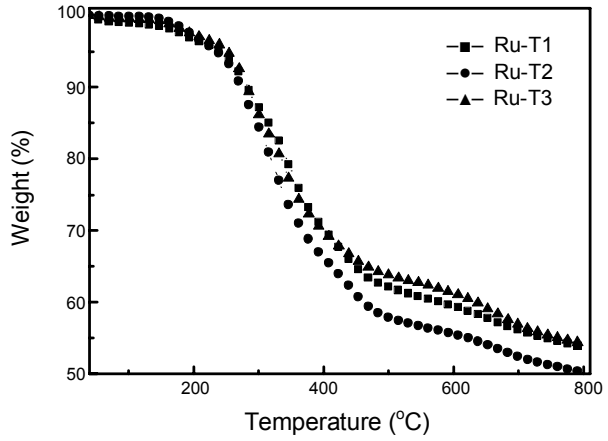

Figure 1. TGA thermograms of Ru-T1, Ru-T2, and Ru-T3.

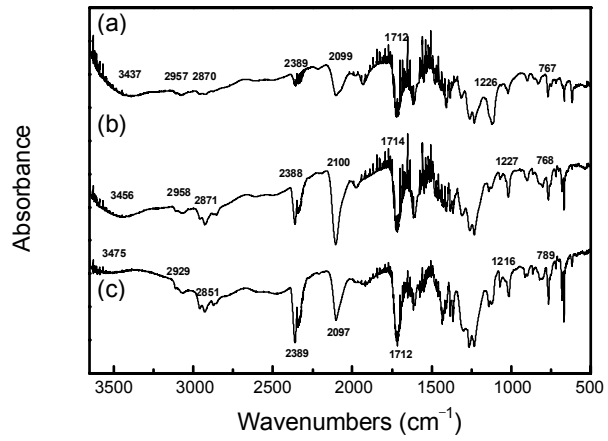

Figure 2. FTIR spectra of Ru-T1 (a), Ru-T2 (b), and Ru-T3 (c), obtained using a solid sample.

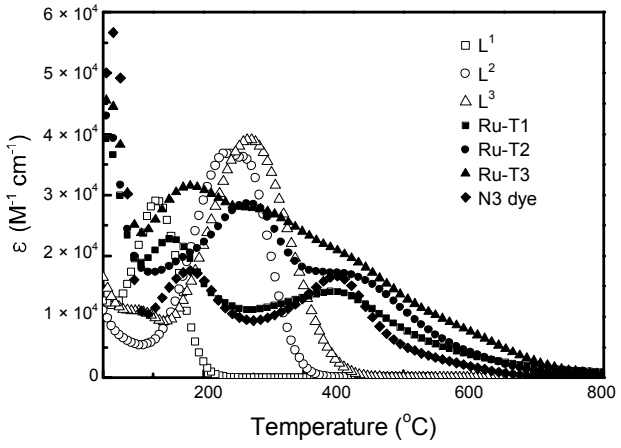

Figure 3. UV-visible absorption spectra of L^1, L^2, L^3, Ru-T1, Ru-T2, Ru-T3, and N3 in DMF.

lic acid groups. The thermal properties of **Ru-T1** ~ **T3** were determined by thermal gravimetric analysis (TGA) under N_2 atmosphere and the TGA thermograms are shown in Figure 1. The TGA thermograms of **Ru-T1** ~ **T3** revealed a 5% weight loss at 224, 231, and 247 °C, respectively.

IR spectroscopy has been shown to be a powerful tool to extract structural information about **Ru-T1** ~ **T3**. Figure 2 shows the typical IR spectra of **Ru-T1** ~ **T3** powders using FTIR in the 3600 - 500 cm^{-1} range. **Ru-T1** ~ **T3** showed a weak and broad band at 3456 cm^{-1} due to carboxylic acid group. The intense bands at 1226, 1227, and 1216 cm^{-1} were assigned to the single-bonded carbon-oxygen in **Ru-T1** ~ **T3**, respectively. The methyl stretching modes were located at 2850 cm^{-1} and 2950 cm^{-1}, together with a weak thiocyanate group at 2389 cm^{-1}. The UV-visible absorption spectra of L^1, L^2, and L^3 in DMF solution are displayed in Figure 3. The λ_{max} values for L^1, L^2, and L^3 were 354, 431, and 452 nm, respectively, which were assigned to the π-π^* transition. The absorption maximum of L^3 was red-shifted by 21 nm compared to L^2, and by 98 nm relative to L^1, which can be attributed to the increasing number of thiophene moieties in L^3. The UV-visible absorption spectra of **Ru-T1** ~ **T3** with **N3** dye are also shown for comparison in Figure 3. The absorption spectrum of **Ru-T1** exhibited three bands centered at 529 nm, 368 nm, and 301 nm. By comparing this spectrum with those of L^1 and the **N3** dye, the absorption bands at 301 nm and 368 nm were assigned to the intra-ligand π-π^* transitions of dcbpy and L^1, respectively. The absorption band at 529 nm is characteristic of the MLCT transition, which is one of the dominant factors for determining the efficiency of sensitizers. The absorption spectrum of **Ru-T2** also presented three bands centered at 551 nm, 445 nm, and 300 nm. The λ_{max} values of the three bands in **Ru-T2** were longer than those of **Ru-T1**, due to the longer conjugation length of ligand in the former. However, the absorption spectrum of **Ru-T3** was different from that of **Ru-T1** and **Ru-T2**. The absorption spectrum of **Ru-T3** revealed two broad bands at 305 nm and 388 nm with a strong tailing at 800 nm due to three thiophene moieties in **Ru-T3**. The absorption and electrochemical properties of **Ru-T1** ~ **T3** and **N3** are summarized in Table 1. The molar absorption coefficients of **Ru-T1** ~ **T3** at the λ_{max} wavelength in solution ranged from 30,400 to 45,600 M^{-1}cm^{-1}. Relatively high molar absorption coefficients can result in high efficiency because of the extended π-electron delocalization. The UV-visible absorption spectra of **Ru-T1** ~ **T3** measured in DMF revealed that the lower energy MLCT band for **Ru-T1** ~ **T3** was centered at 529, 551 and 558 nm with a molar absorption coefficient of 14.1, 16.8 and 27.6 ($\times 10^3$ M^{-1}cm^{-1}), respectively, and N3 (16.6 $\times 10^3$ M^{-1}cm^{-1} at 533 nm) for comparison. The result suggests that the conjugation length of the ligand will affect the MLCT energy between the metal center and the anchoring ligand. We therefore expected that the MLCT transition would be driven to a lower energy due to the extended conjugation length of the ligand in the metal complex, and that use of ruthenium sensitizers would produce a DSSC with a high photovoltaic performance. The higher light harvesting efficiency of **Ru-T3** compared with **Ru-T1** and **Ru-T2** was attributed to the extended conjugation length of the ligand in the thiophene moiety.

CV was used to investigate the electrochemical behavior of **Ru-T1** ~ **T3** and the HOMO and LUMO energy levels. The oxidation potentials of **Ru-T1** ~ **T3** complexes were well correlated with those of the respective donor groups, thiophene, bithiophene, and terthiophene. The HOMO values were calculated from E_{ox} as −5.01, −4.87, and −4.86 eV for **Ru-T1**, **Ru-T2**, and **Ru-T3**, respectively. The LUMO energy level of

Table 1. Absorption and electrochemical data of Ru-T1, Ru-T2, Ru-T3, and N3.

Complex	Absorption coefficient [$*10^3 M^{-1}cm^{-1}$]			HOMO / LUMO [eV][a]
	ε_1 (λ_{max1})	ε_2 (λ_{max2})	ε_3 (λ_{max3})	
N3	56.7 (311 nm)	17.5 (386 nm)	16.6 (532 nm)	-5.52 / -3.84
Ru-T1	30.4 (301 nm)	22.8 (368 nm)	14.1 (529 nm)	-5.01 / -3.05
Ru-T2	43.4 (300 nm)	28.8 (445 nm)	16.8 (551 nm)	-4.87 / -2.95
Ru-T3	45.6 (305 nm)	31.5 (388 nm)	27.6 (563 nm)	-4.86 / -2.95

[a]HOMO is determined from onset of oxidation potentials and LUMO is calculated from HOMO and band gap, which is derived from the absorption onset wavelength.

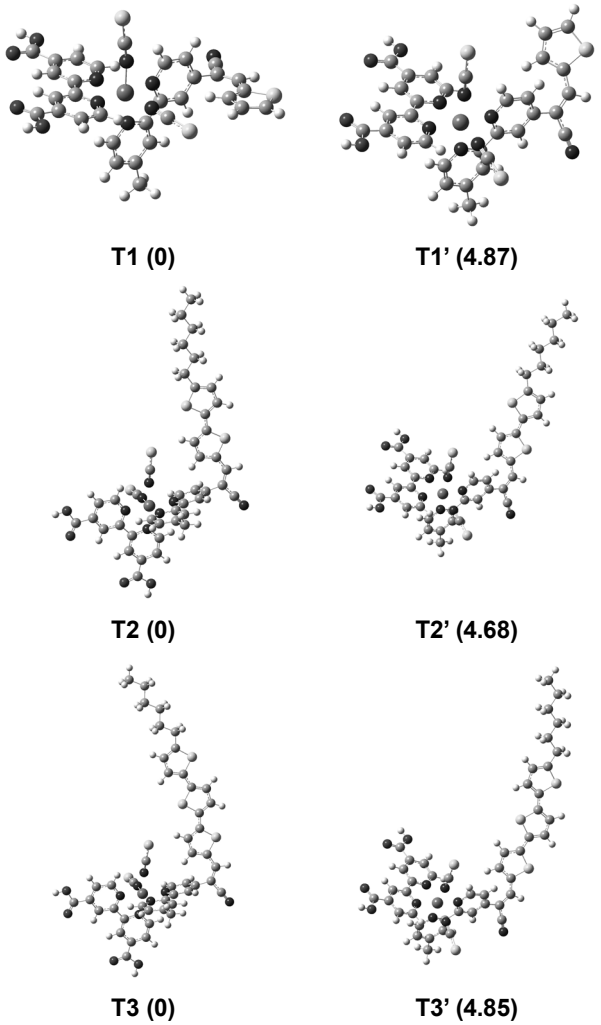

Figure 4. B3LYP/3-21G* optimized structures for L^1, L^2, and L^3. The values in the parentheses are relative stabilities with respect to the T conformers.

Ru-T1, **Ru-T2**, and **Ru-T3** was approximated by subtracting the optical band gap from the HOMO value and these values are listed in Table 1. The results confirmed the thermodynamic favorability of electron injection from the excited **Ru-T1** ~ **T3** sensitizers into the conduction band of TiO_2.[21]

The geometry optimization for the three synthesized L^1, L^2, and L^3 are carried out by the density functional theory (DFT) calculations employing the Becke's three parameters employing Lee-Yang-Parr exchange functional (B3LYP) with 3-21 G* basis sets using a suite of Gaussian 03 programs.[17] Each compound can be classified into two conformations depending on the orientation of the thiophene moieties. More precisely, for all L^1, L^2, and L^3, the T/T' compound denotes the complex, in which the NCS and the thiophene ligand are arranged in different/same direction as shown in Figure 4. The T conformers of L^1, L^2, and L^3 were more stable than the T' conformers by 4.68 ~ 4.87 kcal/mol. This stability difference was primarily attributed to two factors: (1) the hydrogen atom in thiophene ring interacts with the sulfur atom of the −N = C = S group and the distance between hydrogen and sulfur atoms is 2.84 Å, (2) the other hydrogen atom located on the pyridine ring plane interacts with the π-electron. These two non-covalent interactions were considered to be important factors for the superior stability of the T conformers over the T' conformers. On the other hand, the energy gap between the HOMO and LUMO levels of the T conformers increased because the HOMO orbital energy decreased due to the hydrogen bonding and π-H interaction. The results from a DFT calculation of **Ru-T1** ~ **T3** are presented in Figure 5. The LUMO was mainly the π* 2,2-bipyridine-4,4'-dicarboxylic acid ligand with a considerable amount of π back-donation from the t_{2g} orbital. The LUMO had sizeable contributions from the carboxylic groups, thereby enhancing the electronic coupling to the TiO_2 conduction band states. The HOMO was from an antibonding interaction between the t2 g orbital of ruthenium and the π-orbital of NCS. The NCS group pointing in the direction of the electrolyte may have facilitated the reduction of the oxidized dye (Ru^{3+}) through reaction with I^-, making it particularly suitable for highly efficient DSSCs. The π-orbitals on the (E)-3-(5-alkyloligothiophen-5-yl)-2-(4'-methyl-2,2'-bipyridin-4-yl)acrylonitrile ligand have a negligible contribution to HOMO.

Figure 6 shows the photocurrent density-voltage (J-V) curves of a SnO_2 : F/TiO_2/**Ru-T1** ~ **T3** dye/liquid electrolyte/Pt devices under AM 1.5 G (100 mW/cm^2). Table 2 summarizes the photovoltaic properties of the DSSCs using **Ru-T1** ~ **T3** and **N3** for comparison. Among the three cells, the cell fabricated with **Ru-T2** had highest efficiency of about 2.84% (V_{oc} = 0.57 V, J_{sc} = 5.3 mA/cm^2, FF = 0.75). Despite the higher molar absorption coefficient of **Ru-T3**, the lower photovoltaic performance of **Ru-T3** was due to the lower solubility and low J_{sc}, which was associated with its bulky ancillary ligand structure and the lesser absorption of **Ru-T3** on the porous nc-TiO_2 electrode, compared to **Ru-T1** and **Ru-T2**. Another factor for low photovoltaic performance was due to the high LUMO energy level of the **Ru-T1** ~ **T3** sensitizers, which results the low thermodynamic driving

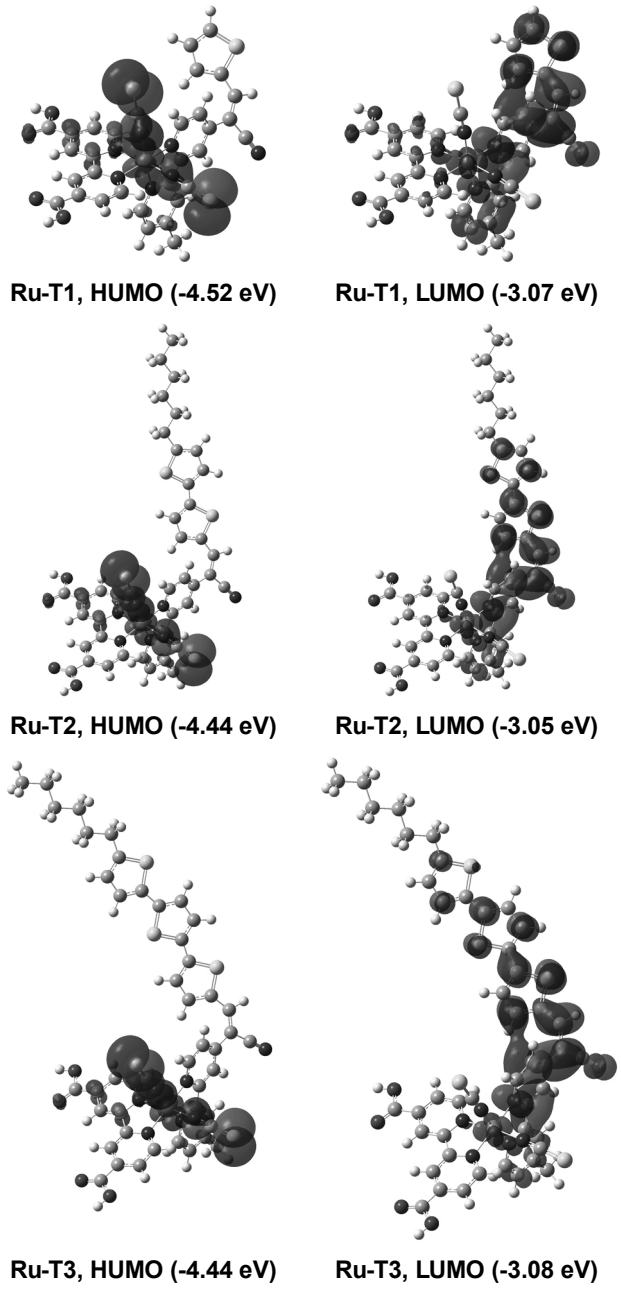

Figure 5. Frontier molecular orbitals of Ru-T1, Ru-T2, and Ru-T3 sensitizers.

force for electron injection from the excited stated LUMO level of **Ru-T1** ~ **T3** sensitizers to the conduction band of TiO_2 relative to N3 dye. Further optimization of the liquid electrolyte components or the introduction of scattering layers should improve the photovoltaic performance of the DSSCs.

Conclusions

We synthesized three novel, heteroleptic ruthenium sensitizers $[Ru(L)(L^x)(NCS)_2]$, where L = 4,4'-bis(carboxylic acid)-2,2'-bipyridine and L^x is (E)-2-(4'-methyl-2,2'-bipyridin-4-yl)-3-(thiophen-2-yl)acrylonitrile or (E)-3-(5'-hexyl-2,2'-bithiophen-5-yl)-2-(4'-methyl-2,2'-bipyridin-4-yl)acrylonitrile or (E)-4-(1-cyano-2-(5"-hexyl-2,2':5',2"-terthiophen-5-yl)-2,2'-bipyridine. We fabricated the DSSCs with a configuration of SnO_2:F/TiO_2/ruthenium dye/liquid electrolyte/Pt devices using these **Ru-T1** ~ **T3** complexes as sensitizers. **Ru-T1** ~ **T3** had a Jsc of 6.0, 5.3 and 4.5 mA/cm^2 and also showed a PCE of 2.45, 2.84 and 1.85% with a Voc of 0.58, 0.57 and 0.54 V, respectively.

Table 2. Photovoltaic parameters of dye-sensitized solar cells with Ru-T1, Ru-T2, Ru-T3 and N3.

Sensitizer	J_{sc} (mA/cm^2)	V_{oc} (V)	Fill Factor (%)	Efficiency (%)	Area (cm^2)
Ru-T1	6.0	0.58	70	2.45	0.21
Ru-T2	5.3	0.57	75	2.84	0.21
Ru-T3	4.5	0.54	76	1.85	0.21
N3	15.1	0.64	67	6.5	0.21

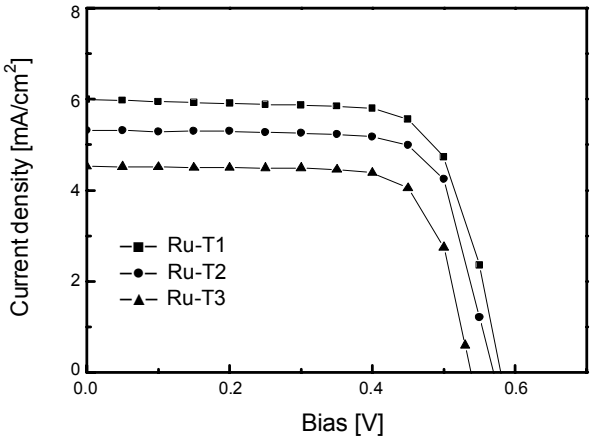

Figure 6. Current density-voltage curves of DSSCs prepared with TiO_2 films impregnated with Ru-T1, Ru-T2, and Ru-T3 in DMF.

Acknowledgments. This work was supported by the Korea Science and Engineering Foundation (KOSEF) grant funded by the Korea government (MEST) (No. 10600000157-06J0000-15710 and R11-2008-088-01-003-0).

References and Notes

1. Bilgen, S.; Kaygusuz, K.; Sari, A. *Energy Sources* **2004**, *26*, 1119.
2. O'Regan, B.; Gratzel, M. *Nature* **1991**, *353*, 737.
3. Nazeeruddin, M. K.; Kay, A.; Rodicio, I.; Humphry-Baker, R.; Muller, E.; Liska, P.; Vlachopoulos, N.; Grätzel, M. *J. Am. Chem. Soc*. **1993**, *115*, 6382.
4. Nazeeruddin, M. K.; Pechy, P.; Renouard, T.; Zakeeruddin, S. M.; Humphry-Baker, R.; Comte, P.; Liska, P.; Cevey, L.; Costa, E.; Shklover, V.; Spiccia, L.; Deacon, G. B.; Bignozzi, C. A.; Grätzel, M. *J. Am. Chem. Soc.* **2001**, *123*, 1613.
5. Ushiroda, S.; Ruzycki, N.; Lu, Y.; Spitler, M. T.; Parkinson, B. A. *J. Am. Chem. Soc*. **2005**, *127*, 5158.
6. Horiuchi, T.; Miura, M.; SumioKa, K.; Uchida, S. *J. Am. Chem. Soc*. **2004**, *126*, 12218.
7. Wang, Z. S.; Yamaguchi, T.; Sugihara, H.; Arakawa, H. *Langmuir* **2005**, *21*, 4272.
8. Nazeeruddin, M. K.; Zakeeruddin, S.; Humphry-Baker, R.; Jirousek, M.; Liska, P.; Vlachopoulos, N.; Shklover, V.; Fischer, C. H.; Grätzel, M. *Inorg. Chem*. **1999**, *38*, 6298.

9. Nazeeruddin, M. K.; Angelis, F. D.; Fantacci, S.; SElloni, A.; Viscardi, G.; Liska, P.; Ito, S.; Takeru, B.; Grätzel, M. *J. Am. Chem. Soc*. **2005**, *127*, 16835.
10. Nazeeruddin, M. K.; Pechy, P.; Grätzel, M. *Chem. Comm*. **1997**, 1705.
11. Yanagida, M.; Singh, L. P.; Sayama, K.; Hara, K.; Katoh, R.; Islam, A.; Sugihara, H.; Arakawa, H.; Nazeeruddin, M. K.; Grätzel, M. *J. Chem. Soc. Dalton Trans*. **2000**, 2817.
12. Sugihara, H.; Singh, L. P.; Sayama, K.; Arakawa, H.; Nazeeruddin, M. K.; Grätzel, M. *Chem. Lett*. **1998**, *10*, 1005.
13. Renouard, T.; Fallahpour, R. A.; Nazeeruddin, M. K.; Humphry-Baker, R.; Gorelsky, S. I.; Lever, A. B. P.; Grätzel, M. *Inorg. Chem*. **2002**, *41*, 367.
14. Wang, P.; Zakeeruddin, S. M.; Moser, J.-E.; Humphry-Baker, R.; Comte, P.; Aranyos, V.; Hagfeldt, A.; Nazeeruddin, M. K.; Grätzel, M. *Adv. Mater*. **2004**, *16*, 1806.
15. Wang, P.; Klein, C.; Humphry-Baker, R.; Comte, P.; Aranyos, V.; Hagfeldt, A.; Nazeeruddin, M. K.; Grätzel, M. *J. Am. Chem. Soc*. **2005**, *127*, 808.
16. Abbotto, A.; Barolo, C.; Bellotto, L.; Angelis, F. D.; Grätzel, M.; Manfredi, N.; Marinzi, C.; Fantacci, S.; Yum, J. H.; Nazeeruddin, M. K. *Chem. Comm*. **2008**, *42*, 5318.
17. Frisch, M. J. *Gaussian 03*, Revision A1; Gaussian Inc.: Pittsburgh, PA, 2003.
18. Kang, M. G.; Kim, K. M.; Ryu, K. S.; Chang, S. H.; Park, N. G.; Hong, J. S.; Kim, K. J. *J. Electrochem. Soc*. **2004**, *151*, E257.
19. Raposo, M. M. M.; Fonseca, A. M. C.; Kirsch, G. *Tetrahedron* **2004**, *60*, 4071.
20. Klein, C.; Nazeeruddin, M. K.; Di Censo, D.; Liska, P.; Grätzel, M. *Inorg. Chem*. **2004**, *43*, 4216.
21. Hagfeldt, A.; Grätzel, M. *Chem. Rev*. **1995**, *95*, 49.